ACS OMEGA

http://pubs.acs.org/journal/acsodf

Article

Poly(vinyl alcohol)-Assisted Exfoliation of van der Waals Materials

Yaodong Li, Shirui Weng, Rui Niu, Weili Zhen, Feng Xu, Wenka Zhu,* and Changjin Zhang*

Cite This: *ACS Omega* 2022, 7, 38774−38781

Read Online

ACCESS | Metrics & More | Article Recommendations | Supporting Information

ABSTRACT: We report a highly efficient and easily transferable poly(vinyl alcohol) (PVA)-assisted exfoliation method, which allows one to obtain van der Waals materials on large scales, e.g., centimeter-scale graphite flakes and hundred-micrometer-scale several layers of $ZnIn_2S_4$ and BN. The present exfoliation scheme is nondestructive, and the materials prepared by PVA-assisted exfoliation can be directly fabricated into devices. This exfoliation approach could be helpful in overcoming the preparation bottleneck for large-scale applications of two-dimensional (2D) materials.

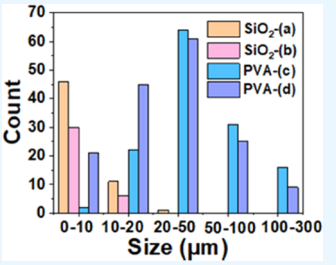

1. INTRODUCTION

Since the successful preparation of graphene,[1] the unique electronic and optoelectronic properties and excellent mechanical properties of two-dimensional (2D) materials have attracted great attention.[2−14] Compared with silicon-based semiconductors, 2D materials have atomically flat surfaces and almost no short-channel effects, which are very promising for next-generation integrated circuits.[15−21] The quality and areas of the films determine the application prospect of 2D materials to a large degree.[22−24] To date, the widely utilized methods for preparing 2D materials are liquid-phase sonication, hydrothermal reactions, chemical vapor deposition (CVD), and mechanical exfoliation.[25−37] However, these methods often have unavoidable drawbacks. For example, it is difficult to control the number of layers in the preparation of 2D materials by liquid-phase sonication, and the surface area of the obtained material is very small.[25,26] The size of the materials synthesized by the hydrothermal method is usually within a few micrometers, the crystalline quality is poor and the thickness is uncontrollable.[27] CVD is a widely used method for synthesizing 2D materials.[28] However, this method introduces some defects, resulting in low crystalline quality and challenges to prepare large-scale films.[29−34] The 2D materials prepared by mechanical exfoliation are of high quality,[35−37] but due to the weak interaction between the layered material and SiO_2,[38] the probability of the material being exfoliated onto the SiO_2 is small, resulting in a very low yield.

By evaporating a layer of gold film on the crystal surface, a large area of material can be peeled off, as a result of the greater interaction between the gold film and the layered material than the van der Waals (vdW) force between the layers.[38] However, cross-sectional transparent electron microscopy characterizations reveal that the deposited gold causes significant defects in the contact materials, such as chemical disorder and Fermi pinning.[23] Further electrical property data also confirm the damage to the materials.[23,39] Such a gold-assisted exfoliation method has been improved in recent years.[40−42] The gold film forms a quasi-covalent bond with the vdW material. However, there is one obvious problem with this approach. That is, the gold film is very difficult to remove,[41] which hinders the direct measurement of electrical properties on gold-bearing substrates. Removal of the gold film with KI/I_2 solution inevitably contaminates or damages 2D materials,[38,40−43] which is contrary to the goal of high quality. For example, KI/I_2 solution can oxidize MoS_2 into MoO_3.[42] In addition, the gold surface needs to be smooth, and it can hardly stay in air for more than 15 min,[42] otherwise there will be no auxiliary stripping effect. To avoid etching by KI/I_2 solution, the hollowed-out gold mesh method was proposed.[43] However, due to the limitation of the hollow mesh structure, the maximum lateral dimension of the exfoliated material is only 15 μm. Moreover, the procedures of gold-assisted exfoliation are quite complicated and the operations are difficult.

Here, we propose an efficient and transfer-friendly poly(vinyl alcohol) (PVA)-assisted exfoliation method, inspired by previous research.[43,44] PVA has a strong bond with the layered material under heating conditions. When the viscosity of PVA is greater than the vdW force of the layered material, the layered material could be effectively peeled off. Since PVA is readily soluble in water, the exfoliated material can be transferred by immersion in deionized water, which is mild and does not damage the sample. Using this method, we can obtain centimeter-scale graphite flakes and hundred-micrometer-scale few layers of $ZnIn_2S_4$ and BN. According to

Received: July 12, 2022
Accepted: October 7, 2022
Published: October 18, 2022

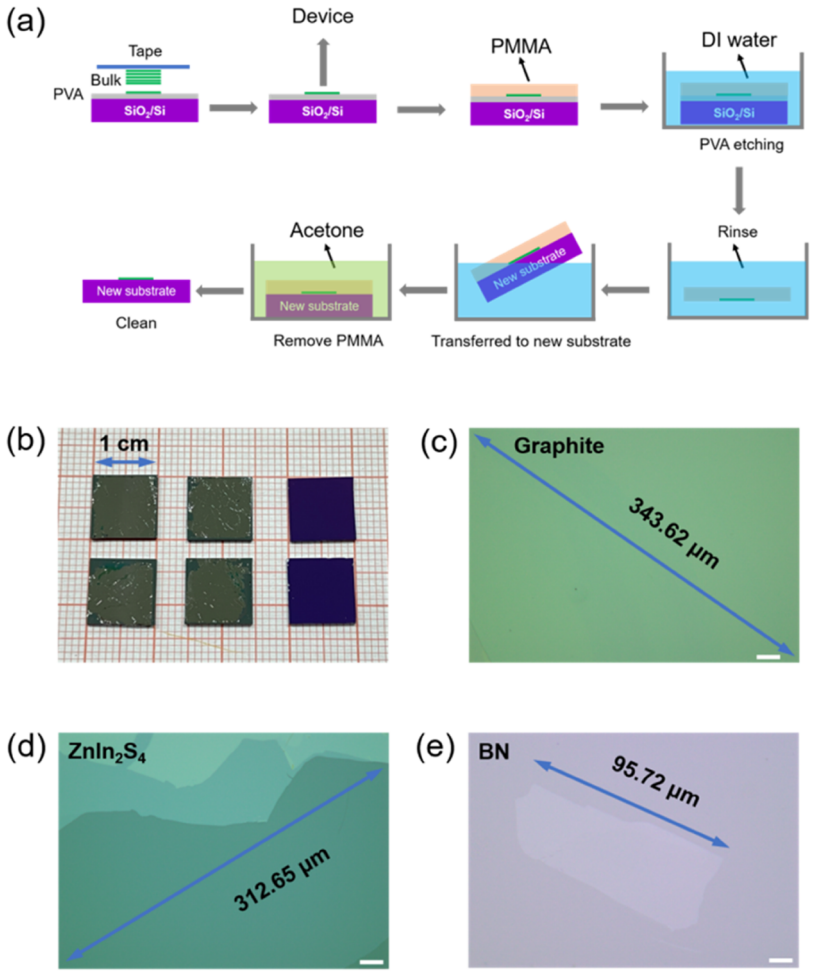

Figure 1. (a) Flow chart of the PVA-assisted exfoliation scheme. (b) Thin graphite sheets transferred to substrates after exfoliation. The left four are obtained from PVA-assisted exfoliation; the right two are on common SiO_2/Si substrates. (c–e) Optical images of (c) PVA-assisted exfoliated graphite flake, (d) $ZnIn_2S_4$ flake, and (e) BN flake. The scale bar in (c) and (d) is 20 μm, and in (e) is 10 μm.

previous reports,[41] the weak adhesion of superflat gold to graphite and BN leads to the mediocre effect of gold-assisted stripping. We deliberately choose graphite and BN to perform the comparative experiments. By comparing the spin-coated PVA substrate with the ordinary SiO_2/Si substrate, the sizes of samples on the PVA substrate are obviously larger than those on the ordinary SiO_2/Si substrate, and the efficiency is much higher, suggesting the advantage of the PVA-assisted exfoliation scheme. In addition, the materials of PVA-assisted exfoliation could be directly fabricated into devices to study electrical properties.[43,45] Raman, X-ray photoelectron spectroscopy (XPS), and electrical characterizations prove that the PVA-assisted exfoliation scheme is nondestructive. Thus the PVA-assisted exfoliation scheme could be very promising in future electronic applications of van der Waals materials.

2. RESULTS

Figure 1a shows the flow chart of PVA-assisted exfoliation of vdW layered materials. First, the SiO_2/Si substrate is ultrasonically cleaned using acetone, isopropanol, and ethanol to remove contaminants from the substrate surface. Then, the SiO_2/Si surface is spin-coated with 8% PVA solution twice and baked on a hot plate at 80 °C for 3 min to cure the PVA solution. The PVA layer is used as an auxiliary peeling medium, and the substrate is named the PVA-SiO_2/Si substrate. According to atomic force microscopy (AFM), the thickness of the PVA film is 1 μm, as shown in Figure S1a in the supplementary information. Here, we take graphite for example. The blue tape is used as a release tape to exfoliate large-sized thick graphite sheets from highly oriented pyrolytic graphite. The blue tape with graphite sheets is attached to the PVA-SiO_2/Si substrate. The tape is slightly pressed to ensure adequate contact between the graphite and the PVA layer. Then the composite is heated on a hot plate at 100 °C for 3 min, and the blue tape is slowly removed. The layered materials is exfoliated onto the PVA-SiO_2/Si substrate, taking advantage of the high adhesion of PVA at high temperature. Centimeter-sized graphite flakes have been stripped down by this technique.

Figure 1b shows that in the four substrates on the left, the graphite flakes cover almost the entire PVA-SiO_2/Si substrate, and the planar size is comparable to that of the graphite bulk material. Figure 1c is the microscopic image of Figure 1b. It can be seen that the peeled graphite flakes are smooth and clean. The high success rate of this technique in exfoliating graphite confirms that the force between PVA and the graphite flakes is greater than the vdW force between the graphite layers. As a comparative experiment, the same procedure was used to clean the SiO_2/Si substrate, but without spin-coating the PVA solution, the abovementioned lift-off operation was

https://doi.org/10.1021/acsomega.2c04409
ACS Omega 2022, 7, 38774−38781

performed. The two substrates on the right panel of Figure 1b show the exfoliation results using ordinary SiO_2/Si substrates. No obvious graphite sheets are found on the substrates, manifesting the advantage of PVA-assisted exfoliation of large-area graphite flakes.

We have also tried to exfoliate other two-dimensional van der Waals materials such as $ZnIn_2S_4$ and BN. Figure 1d shows several layers of $ZnIn_2S_4$ with lateral dimensions of over 300 μm. Figure 1e shows several layers of BN with lateral dimensions also approaching 100 μm. It is demonstrated that PVA-assisted exfoliation is an effective technique for large-area exfoliation of vdW layered materials.

In addition to the capability to peel off large samples, the method also has the characteristics of easy transfer and no damage to the material. Since PVA is easily soluble in water, the materials prepared on the PVA-SiO_2/Si substrate is spin-coated with poly(methyl methacrylate) (PMMA) solution and then immersed in deionized water to dissolve the PVA layer between the sample and the substrate, making the PMMA with the material float in water [Figure 1a]. Transfer of the sample is completed by scooping it out with a new substrate and soaking it in acetone to remove PMMA. Note that if the exfoliated 2D materials are visible to the naked eye, the PVA can be dissolved directly in deionized water without spin-coating the PMMA solution. The types of new substrates are not limited, such as SiO_2/Si, sapphire, poly(ethylene terephthalate) (PET), polyimide (PI), etc., so this process can also make flexible electronic devices. In contrast, ordinary SiO_2/Si substrates need to be etched with strong acid or alkali to etch the SiO_2 layer after stripping. As is known, etching with a strong acid or alkali is notoriously difficult and, if wrong, can cause irreversible damage. The gold-assisted exfoliation technique uses a KI/I_2 solution to etch the gold film. In practice, the etching rate is very slow.

To further demonstrate the efficiency of PVA-assisted exfoliation and investigate the adhesion between the PVA layer and the vdW layered material, comparative experiments of exfoliated BN on PVA-SiO_2/Si and ordinary SiO_2/Si substrates are carried out. According to our previous experience, BN is more difficult to exfoliate than some materials such as graphite and $SnSe_2$, thus the example of BN is somewhat representative. We violently dissociate BN with blue tape, so that a large number of BN fragments adhere to the blue tape. Four additional pieces of adhesive tape are applied to the tape with the same force once and then peeled off. Microscopic observation of the BN flakes on the 4 torn tapes reveals little difference in their number and size. Then two blue tapes are randomly picked and attached to two PVA-SiO_2/Si substrates, and the other two are pasted on two ordinary SiO_2/Si substrates. Thermal mechanical exfoliation is then carried out, as described in the Methods section.

Figure 2a–d shows the images of ordinary SiO_2/Si and PVA-SiO_2/Si substrates, respectively. It can be seen that the peeling effect of PVA-SiO_2/Si substrates is obviously better than that of ordinary SiO_2/Si substrates. For comparison, the size and number of BN obtained from the two types of substrates are counted, and the statistical results are shown in Figure 2f. The amount of BN on the PVA-SiO_2/Si substrates is more than eight times that on the SiO_2/Si substrates. Meanwhile, the size of BN on the PVA-SiO_2/Si substrates is much larger. On SiO_2/Si substrates, 81% of BN flakes are smaller than 10 μm in size. On PVA-SiO_2/Si substrates, only 8% of BN has a size below 10 μm and 28% of BN has a size

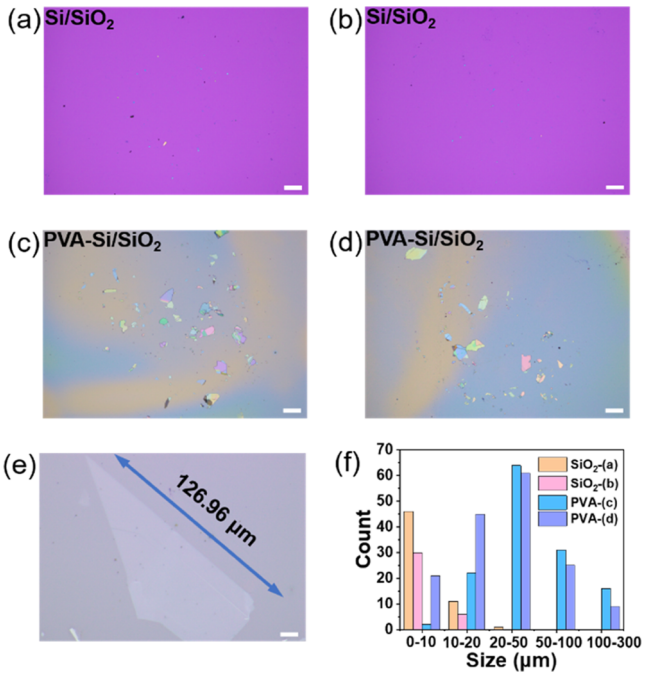

Figure 2. (a, b) Typical optical images of BN exfoliated on SiO_2/Si substrates. (c, d) Optical images of PVA-assisted exfoliated BN. (e) A large flake of exfoliated BN. The scale bar in (a–d) is 200 μm, and the scale bar in (e) is 10 μm. (f) Histogram of peeling effect statistics.

above 50 μm. The distribution of BN is close to the original pattern on the tape, confirming the high efficiency of PVA-assisted transfer. Turning the microscope to high magnification, it can be seen that there are hundred-micrometer-scaled BN on the PVA-SiO_2/Si substrates, as shown in Figure 2e, which is not found on the ordinary SiO_2/Si substrates. After BN on the PVA-SiO_2/Si substrate is transferred, one piece is selected for Raman characterization. As shown in Figure S2 in the supplementary information, the characteristic peak E_{2g} of BN is at 1367 cm^{-1}, which is consistent with the literature.[46]

Raman spectroscopy is an important tool for characterizing materials and can measure the crystal structure and crystalline quality of crystals. Therefore, graphite flakes prepared by PVA-assisted exfoliation are examined for defect information by Raman spectroscopy. The graphite flakes are removed from the PVA-SiO_2/Si substrate and transferred to a new SiO_2/Si substrate. Raman spectra of the same region of the sample are measured before and after transfer. As shown in Figure 3a, both Raman spectra reveal no Raman peaks in the D-band, indicating that there are almost no transfer-induced defects in the graphite flakes. In the Raman spectrum before transfer the positions of the G peak and 2D peak are 1581 and 2719 cm^{-1}, respectively, which are consistent with previous reports.[47] After the transfer, the Raman spectrum almost completely overlaps with the former, indicating that the crystal quality of the graphite flakes does not change after the transfer and the PVA-assisted exfoliation technique does not damage the samples.

X-ray photoemission spectroscopy (XPS) experiments are performed to characterize the chemical composition, valence states, and molecular structures of the samples. In the past, it was difficult to use XPS for characterization due to the small size of mechanically exfoliated samples. However, our samples are large enough for XPS characterization. Figure 3b shows the survey spectra before and after transfer and after vacuum annealing at 300 °C. Compared with the spectrum before

https://doi.org/10.1021/acsomega.2c04409
ACS Omega 2022, 7, 38774–38781

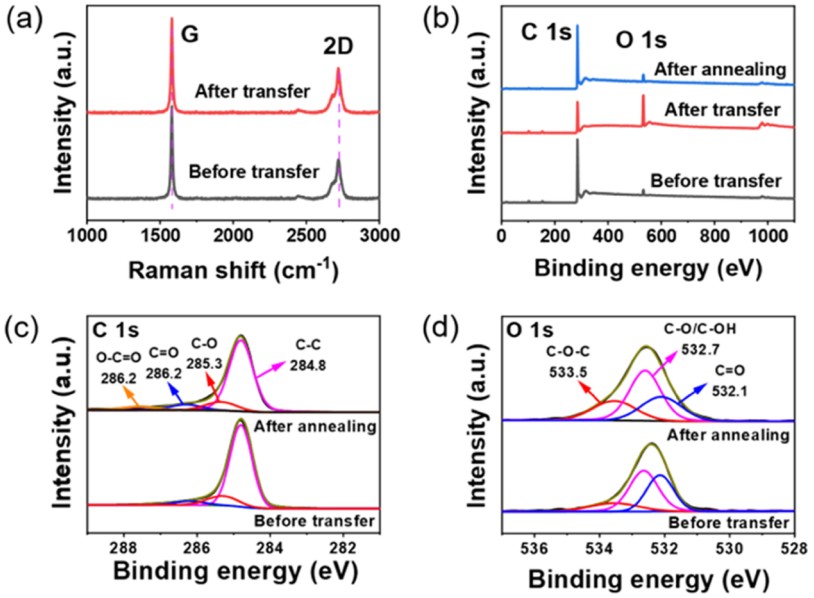

Figure 3. (a) Raman spectra of a PVA-assisted exfoliated graphite flake before and after transfer. (b) XPS survey spectra before transfer, after transfer, and after annealing. (c) Detailed view of the C 1s peak and the fitting results before transfer (lower) and after (upper) annealing. (d) O 1s peak and the fitting results before transfer (lower) and after (upper) annealing.

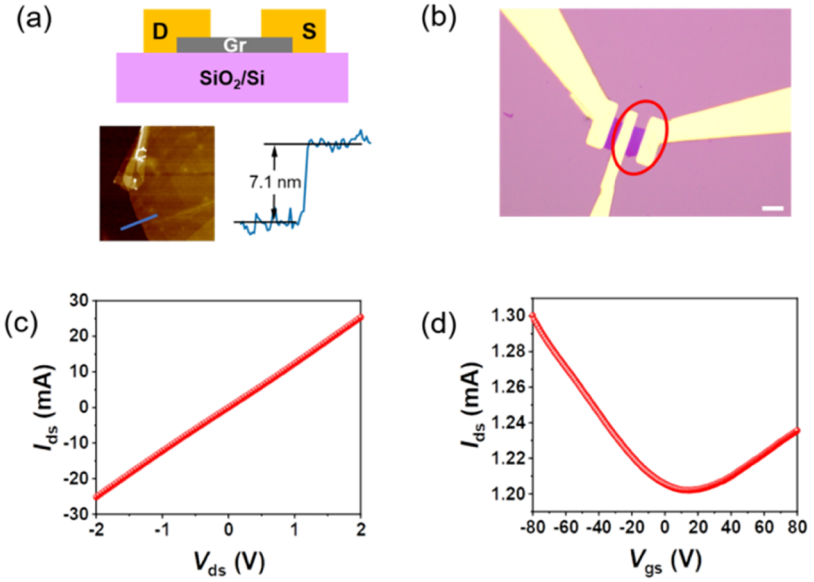

Figure 4. (a) Upper panel: Schematic diagram of a transferred graphene device. Lower panel: AFM image and height profile of a piece of graphene sample, which indicates that the thickness of the sample is 7.1 nm. (b) Optical image of the device. The scale bar is 10 μm. (c) I_{ds}−V_{ds} curve showing a metallic character. (d) FET transfer curve taken at V_{ds} = 0.1 V.

transfer a prominent O peak is observed in the spectrum after transfer. This phenomenon should be attributed to the added moisture during the dissolution of PVA. The O peak is suppressed if the sample is annealed under vacuum conditions, which confirms the hypothesis. A detailed peak fit of the C and O peaks is performed and shown in Figure 3c, d. In Figure 3c, the main peak at 284.8 eV represents the C−C bond of sp^2 hybridization,[48] which does not shift after the transfer. In Figure 3d, the nearly identical results show that the annealing process can effectively remove moisture from the samples.

We have also investigated the electrical properties of graphene prepared by this technique. Field effect transistor (FET) devices were fabricated on the exfoliated and transferred graphene on a SiO_2/Si substrate with a 300 nm oxide layer. Cr/Au with a thickness of 10/90 nm was used as the source−drain electrodes, and the SiO_2 layer was used as the gate dielectric. The device has a channel length of 5.8 μm and a channel width of 13.7 μm. The schematic diagram of the device is shown in the upper part of Figure 4a, and the optical image is shown in Figure 4b. The thickness of graphene measured by AFM is 7.1 nm, as shown in the lower part of Figure 4a. Figure 4c shows the I_{ds}−V_{ds} characteristic curve of the device. The curve passes through the origin and is completely symmetrical, indicating that the Cr/Au electrodes form an ohmic contact with graphene. Figure 4d shows the FET transfer curve of the device, which is consistent with the metallic nature of graphene.[49] According to the formula

https://doi.org/10.1021/acsomega.2c04409
ACS Omega 2022, 7, 38774−38781

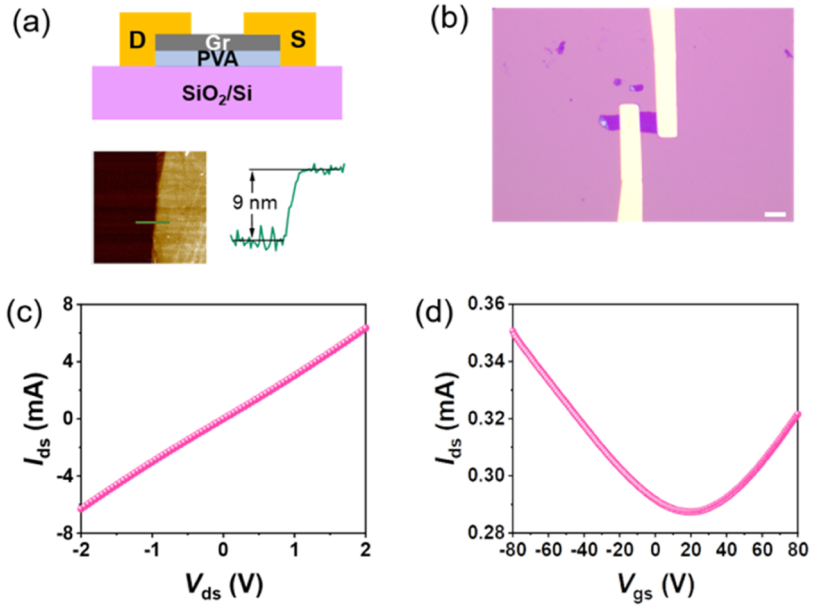

Figure 5. (a) Upper panel: Schematic diagram of a graphene device directly fabricated on a 1% PVA-SiO_2/Si substrate. Lower panel: AFM image and height profile. (b) Optical image of the device. The scale bar is 10 μm. (c) I_{ds}−V_{ds} curve. (d) FET transfer curve taken at V_{ds} = 0.1 V.

$\mu = \frac{dI_{ds}}{dV_{gs}} \times \frac{L}{WV_{ds}C_i}$, where μ is the carrier mobility, L is the channel length, W is the channel width, C_i is the oxide layer capacitance per unit area, the carrier mobility can be calculated as 271.5 $cm^2\ V^{-1}\ s^{-1}$.

From the XPS survey spectra in Figure 3b, it can be seen that there are small amounts of moisture left on the surface of the graphite sheets after the wet transfer. Moisture has a substantial influence on the performance of low-dimensional devices. To remove moisture, the graphene device is carefully annealed under vacuum conditions. The electrical performance of the device could be greatly improved by annealing, transfer electrode, BN packaging, and edge contact.[39,50−55]

Due to the insulating nature of the PVA film,[45] the materials prepared by the PVA-assisted exfoliation method can directly fabricate electronic devices on the PVA-SiO_2/Si substrate without transfer. This etch-free process is gentle and convenient. In contrast, the samples prepared by gold-assisted exfoliation cannot be directly used for device fabrication. A 1% concentration of PVA solution is chosen, spin-coated only once on the SiO_2/Si substrate, and dried on a heating pad. The thickness characterized by AFM is 24 nm, as shown in Figure S1c in the Supporting Information. Encouragingly, although the thickness of the 1% PVA layer is much smaller than that of the 8% PVA layer, the auxiliary exfoliation effect still works well due to the minor roughness of the PVA layer and its adhesion. Only the edge of the PVA in the lower part of the sample is dissolved due to the cover protection of graphene. PVA is an insulating polymer with a dielectric constant of 6.3, which can be used as a gate dielectric.[43,45] Therefore the lithography process is carried out directly on the surface using PVA/SiO_2 as the gate dielectric. The schematic diagram of the device is shown in the upper panel of Figure 5a and the optical image is shown in Figure 5b. The electrical measurement results are shown in Figure 5c,d. Except for the magnitude of source−drain currents, the characteristic curve and the transfer cure are almost the same as those obtained on the bare SiO_2/Si substrate. This demonstrates the ability of PVA-covered substrate to directly fabricate the electronic devices, which greatly simplifies the process of device fabrication. It should be pointed out that in the present work, we can only exfoliate multilayer van der Waals materials such as graphite and BN. It is hopeful that in near future, the PVA-assisted exfoliation scheme could be widely utilized to fabricate electronic devices made of various van der Waals materials with thickness down to a monolayer.

3. CONCLUSIONS

In summary, we report a highly efficient and transfer-friendly PVA-assisted exfoliation method for the exfoliation of van der Waals materials. PVA has a strong bond with the layered material under heating conditions, which allows for the exfoliation of large-area samples. Since PVA is readily soluble in water, the exfoliated material can be transferred by immersion in deionized water, which is mild and does not damage the sample. Using this method, we obtained centimeter-scale graphite flakes and hundred-micrometer-scale few layers of $ZnIn_2S_4$ and BN. The Raman, XPS, and electrical characterizations prove that the new exfoliation scheme is nondestructive. Moreover, materials prepared by PVA-assisted exfoliation can be directly fabricated into devices, which greatly simplifies the process of device fabrication.

4. METHODS

4.1. Crystals. BN crystals and graphite crystals were brought commercially from the Xianfeng Nano Company. $ZnIn_2S_4$ crystals were grown by a chemical vapor transport method. The growth conditions were described preciously.[56]

4.2. Exfoliation. The SiO_2/Si substrate was placed in a sonicator, followed by ultrasonic cleaning with acetone, isopropanol, and ethanol for 5 minutes, and dried with nitrogen. The PVA solution of 8 wt % concentration (Aladdin, molecular weight ∼205000) was prepared and spin-coated on the SiO_2/Si substrate at 4000 rpm for 60 s. Spin-coating was performed twice, cured at 80 °C for 3 min each time, and the resulting substrate was named the PVA-SiO_2/Si substrate. The single crystal was repeatedly peeled off several times with blue

https://doi.org/10.1021/acsomega.2c04409
ACS Omega 2022, 7, 38774−38781

tape and attached to the PVA-SiO_2/Si substrate. Slight pressure was applied so that the layered material on the tape was in full contact with the PVA layer. The PVA-SiO_2/Si substrate was then heated at 100 °C for 3 min, and the blue tape was slowly lifted, leaving a large amount of layered material on the PVA-SiO_2/Si substrate. In the control group, the blue tape was directly attached to the cleaned SiO_2/Si substrate. In addition to the 8 wt % concentration PVA solution, a 1 wt % concentration PVA solution was also prepared following the same procedure.

4.3. Etching. The etching process was performed using a typical wet transfer method. Namely, the PMMA solution was spin-coated on the substrate and cured at 80 °C for 3 min. The PVA-SiO_2/Si substrate attached with samples was immersed in deionized water and heated on a hot plate (70 °C) to increase the rate at which deionized water dissolved the PVA. In the control group, the SiO_2 layer was etched with HF solution.

4.4. Characterization, Fabrication, and Measurements. Optical images of materials and devices were taken using an Olympus BX53M microscope. The thickness of thin flakes was characterized on a Bruker Dimension Icon atomic force microscopy system. The Raman spectra were recorded on a confocal Raman spectrometer (Renishaw inVia Reflex) with a laser wavelength of 532 nm. Laser direct writing lithography was performed using a DaLI maskless lithography system. A thermal evaporation coater was used for the deposition of electrode metals. The electrical measurements were carried out on a probe station combined with a Keithley 2636B source meter.

■ ASSOCIATED CONTENT

Supporting Information

The Supporting Information is available free of charge at https://pubs.acs.org/doi/10.1021/acsomega.2c04409.

AFM images of the PVA layers (Figure S1) and the Raman spectrum of BN obtained by PVA-assisted exfoliation, and transferred to a new substrate (Figure S2) (PDF)

■ AUTHOR INFORMATION

Corresponding Authors

Wenka Zhu − *High Magnetic Field Laboratory of Anhui Province, Hefei Institutes of Physical Science, Chinese Academy of Sciences, Hefei 230031, China;* orcid.org/0000-0003-4312-7012; Email: wkzhu@hmfl.ac.cn

Changjin Zhang − *High Magnetic Field Laboratory of Anhui Province, Hefei Institutes of Physical Science, Chinese Academy of Sciences, Hefei 230031, China; Institutes of Physical Science and Information Technology, Anhui University, Hefei 230601, China;* orcid.org/0000-0003-1464-1741; Email: zcjin@ustc.edu.cn

Authors

Yaodong Li − *High Magnetic Field Laboratory of Anhui Province, Hefei Institutes of Physical Science, Chinese Academy of Sciences, Hefei 230031, China; University of Science and Technology of China, Hefei 230026, China*

Shirui Weng − *High Magnetic Field Laboratory of Anhui Province, Hefei Institutes of Physical Science, Chinese Academy of Sciences, Hefei 230031, China*

Rui Niu − *High Magnetic Field Laboratory of Anhui Province, Hefei Institutes of Physical Science, Chinese Academy of Sciences, Hefei 230031, China*

Weili Zhen − *High Magnetic Field Laboratory of Anhui Province, Hefei Institutes of Physical Science, Chinese Academy of Sciences, Hefei 230031, China*

Feng Xu − *High Magnetic Field Laboratory of Anhui Province, Hefei Institutes of Physical Science, Chinese Academy of Sciences, Hefei 230031, China*

Complete contact information is available at: https://pubs.acs.org/10.1021/acsomega.2c04409

Notes

The authors declare no competing financial interest.

■ ACKNOWLEDGMENTS

This work was supported by the National Key R&D Program of China (Grant No. 2021YFA1600201) and the National Natural Science Foundation of China (Grant Nos. 11874363, 11974356, and U1932216).

■ REFERENCES

(1) Novoselov, K. S.; Geim, A. K.; Morozov, S. V.; Jiang, D.; Zhang, Y.; Dubonos, S. V.; Grigorieva, I. V.; Firsov, A. A. Electric field effect in atomically thin carbon films. *Science* **2004**, *306*, 666−669.

(2) Xia, F.; Wang, H.; Xiao, D.; Dubey, M.; Ramasubramaniam, A. Two-dimensional material nanophotonics. *Nat. Photonics* **2014**, *8*, 899−907.

(3) Wang, Q. H.; Kalantar-Zadeh, K.; Kis, A.; Coleman, J. N.; Strano, M. S. Electronics and optoelectronics of two-dimensional transition metal dichalcogenides. *Nat. Nanotechnol.* **2012**, *7*, 699−712.

(4) Kim, S.; Konar, A.; Hwang, W. S.; Lee, J. H.; Lee, J.; Yang, J.; Jung, C.; Kim, H.; Yoo, J. B.; Choi, J. Y.; Jin, Y. W.; Lee, S. Y.; Jena, D.; Choi, W.; Kim, K. High-mobility and low-power thin-film transistors based on multilayer MoS_2 crystals. *Nat. Commun.* **2012**, *3*, No. 1011.

(5) Yin, Z.; Li, H.; Li, H.; Jiang, L.; Shi, Y.; Sun, Y.; Lu, G.; Zhang, Q.; Chen, X.; Zhang, H. Single-layer MoS_2 phototransistors. *ACS Nano* **2012**, *6*, 74−80.

(6) Yi, Y.; Sun, Z.; Li, J.; Chu, P. K.; Yu, X. F. Optical and Optoelectronic Properties of Black Phosphorus and Recent Photonic and Optoelectronic Applications. *Small Methods* **2019**, *3*, No. 1900165.

(7) Qiu, Q.; Huang, Z. Photodetectors of 2*D* Materials from Ultraviolet to Terahertz Waves. *Adv. Mater.* **2021**, *33*, No. 2008126.

(8) Bernardi, M.; Palummo, M.; Grossman, J. C. Extraordinary sunlight absorption and one nanometer thick photovoltaics using two-dimensional monolayer materials. *Nano Lett.* **2013**, *13*, 3664−3670.

(9) Wang, H.; Li, Z.; Li, D.; Chen, P.; Pi, L.; Zhou, X.; Zhai, T. Van der Waals Integration Based on Two-Dimensional Materials for High-Performance Infrared Photodetectors. *Adv. Funct. Mater.* **2021**, *31*, No. 2103106.

(10) Koppens, F. H. L.; Mueller, T.; Avouris, P.; Ferrari, A. C.; Vitiello, M. S.; Polini, M. Photodetectors based on graphene, other two-dimensional materials and hybrid systems. *Nat. Nanotechnol.* **2014**, *9*, 780−793.

(11) Tamulewicz, M.; Kutrowska-Girzycka, J.; Gajewski, K.; Serafinczuk, J.; Sierakowski, A.; Jadczak, J.; Bryja, L.; Gotszalk, T. P. Layer number dependence of the work function and optical properties of single and few layers MoS_2: effect of substrate. *Nanotechnology* **2019**, *30*, No. 245708.

(12) Akinwande, D.; Brennan, C. J.; Bunch, J. S.; Egberts, P.; Felts, J. R.; Gao, H.; Huang, R.; Kim, J.-S.; Li, T.; Li, Y.; Liechti, K. M.; Lu, N.; Park, H. S.; Reed, E. J.; Wang, P.; Yakobson, B. I.; Zhang, T.; Zhang, Y.-W.; Zhou, Y.; Zhu, Y. A review on mechanics and

mechanical properties of 2D materials—Graphene and beyond. *Extreme Mech. Lett.* **2017**, *13*, 42−77.
(13) Kim, J. H.; Jeong, J. H.; Kim, N.; Joshi, R.; Lee, G.-H. Mechanical properties of two-dimensional materials and their applications. *J. Phys. D: Appl. Phys.* **2019**, *52*, No. 083001.
(14) Zhang, J.; Huang, Y.; Tan, Z.; Li, T.; Zhang, Y.; Jia, K.; Lin, L.; Sun, L.; Chen, X.; Li, Z.; Tan, C.; Zhang, J.; Zheng, L.; Wu, Y.; Deng, B.; Chen, Z.; Liu, Z.; Peng, H. Low-Temperature Heteroepitaxy of 2D PbI_2 /Graphene for Large-Area Flexible Photodetectors. *Adv. Mater.* **2018**, *30*, No. 1803194.
(15) Zeng, M.; Xiao, Y.; Liu, J.; Yang, K.; Fu, L. Exploring Two-Dimensional Materials toward the Next-Generation Circuits: From Monomer Design to Assembly. *Chem. Rev.* **2018**, *118*, 6236−6296.
(16) Xie, L.; Liao, M.; Wang, S.; Yu, H.; Du, L.; Tang, J.; Zhao, J.; Zhang, J.; Chen, P.; Lu, X.; Wang, G.; Xie, G.; Yang, R.; Shi, D.; Zhang, G. Graphene-Contacted Ultrashort Channel Monolayer MoS_2 Transistors. *Adv. Mater.* **2017**, *29*, No. 1702522.
(17) Wang, S.; Liu, X.; Zhou, P. The Road for 2D Semiconductors in the Silicon Age. *Adv. Mater.* **2022**, *34*, No. 2106886.
(18) Das, S.; Sebastian, A.; Pop, E.; McClellan, C. J.; Franklin, A. D.; Grasser, T.; Knobloch, T.; Illarionov, Y.; Penumatcha, A. V.; Appenzeller, J.; Chen, Z.; Zhu, W.; Asselberghs, I.; Li, L.-J.; Avci, U. E.; Bhat, N.; Anthopoulos, T. D.; Singh, R. Transistors based on two-dimensional materials for future integrated circuits. *Nat. Electron.* **2021**, *4*, 786−799.
(19) Su, S. K.; Chuu, C. P.; Li, M. Y.; Cheng, C. C.; Wong, H. S. P.; Li, L. J. Layered Semiconducting 2D Materials for Future Transistor Applications. *Small Struct.* **2021**, *2*, No. 2000103.
(20) Desai, S. B.; Madhvapathy, S. R.; Sachid, A. B.; Llinas, J. P.; Wang, Q.; Ahn, G. H.; Pitner, G.; Kim, M. J.; Bokor, J.; Hu, C.; Wong, H. P.; Javey, A. MoS_2 transistors with 1-nanometer gate lengths. *Science* **2016**, *354*, 99−102.
(21) Liu, L.; Kong, L.; Li, Q.; He, C.; Ren, L.; Tao, Q.; Yang, X.; Lin, J.; Zhao, B.; Li, Z.; Chen, Y.; Li, W.; Song, W.; Lu, Z.; Li, G.; Li, S.; Duan, X.; Pan, A.; Liao, L.; Liu, Y. Transferred van der Waals metal electrodes for sub-1-nm MoS_2 vertical transistors. *Nat. Electron.* **2021**, *4*, 342−347.
(22) Hong, S.; Zagni, N.; Choo, S.; Liu, N.; Baek, S.; Bala, A.; Yoo, H.; Kang, B. H.; Kim, H. J.; Yun, H. J.; Alam, M. A.; Kim, S. Highly sensitive active pixel image sensor array driven by large-area bilayer MoS_2 transistor circuitry. *Nat. Commun.* **2021**, *12*, No. 3559.
(23) Liu, Y.; Guo, J.; Zhu, E.; Liao, L.; Lee, S. J.; Ding, M.; Shakir, I.; Gambin, V.; Huang, Y.; Duan, X. Approaching the Schottky-Mott limit in van der Waals metal-semiconductor junctions. *Nature* **2018**, *557*, 696−700.
(24) Sun, B.; Pang, J.; Cheng, Q.; Zhang, S.; Li, Y.; Zhang, C.; Sun, D.; Ibarlucea, B.; Li, Y.; Chen, D.; Fan, H.; Han, Q.; Chao, M.; Liu, H.; Wang, J.; Cuniberti, G.; Han, L.; Zhou, W. Synthesis of Wafer-0129-8Mott limit in van der Waals Deposition for Electronic Device Applications. *Adv. Mater. Technol.* **2021**, *6*, No. 2000744.
(25) Coleman, J. N.; Lotya, M.; O'Neill, A.; Bergin, S. D.; King, P. J.; Khan, U.; Young, K.; Gaucher, A.; De, S.; Smith, R. J.; Shvets, I. V.; Arora, S. K.; Stanton, G.; Kim, H. Y.; Lee, K.; Kim, G. T.; Duesberg, G. S.; Hallam, T.; Boland, J. J.; Wang, J. J.; Donegan, J. F.; Grunlan, J. C.; Moriarty, G.; Shmeliov, A.; Nicholls, R. J.; Perkins, J. M.; Grieveson, E. M.; Theuwissen, K.; McComb, D. W.; Nellist, P. D.; Nicolosi, V. Two-dimensional nanosheets produced by liquid exfoliation of layered materials. *Science* **2011**, *331*, 568−571.
(26) Niu, L.; Coleman, J. N.; Zhang, H.; Shin, H.; Chhowalla, M.; Zheng, Z. Production of Two-Dimensional Nanomaterials via Liquid-Based Direct Exfoliation. *Small* **2016**, *12*, 272−293.
(27) Ou, J. Z.; Ge, W.; Carey, B.; Daeneke, T.; Rotbart, A.; Shan, W.; Wang, Y.; Fu, Z.; Chrimes, A. F.; Wlodarski, W.; Russo, S. P.; Li, Y. X.; Kalantar-Zadeh, K. Physisorption-Based Charge Transfer in Two-Dimensional SnS_2 for Selective and Reversible NO_2 Gas Sensing. *ACS Nano* **2015**, *9*, 10313−10323.
(28) Kim, S. Y.; Kwak, J.; Ciobanu, C. V.; Kwon, S. Y. Recent Developments in Controlled Vapor-Phase Growth of 2D Group 6 Transition Metal Dichalcogenides. *Adv. Mater.* **2019**, *31*, No. 1804939.
(29) Zhang, X.; Liao, Q.; Kang, Z.; Liu, B.; Liu, X.; Ou, Y.; Xiao, J.; Du, J.; Liu, Y.; Gao, L.; Gu, L.; Hong, M.; Yu, H.; Zhang, Z.; Duan, X.; Zhang, Y. Hidden Vacancy Benefit in Monolayer 2D Semiconductors. *Adv. Mater.* **2021**, *33*, No. 2007051.
(30) Chae, W. H.; Cain, J. D.; Hanson, E. D.; Murthy, A. A.; Dravid, V. P. Substrate-induced strain and charge doping in CVD-grown monolayer MoS_2. *Appl. Phys. Lett.* **2017**, *111*, No. 143106.
(31) Liu, H.; Zhu, Y.; Meng, Q.; Lu, X.; Kong, S.; Huang, Z.; Jiang, P.; Bao, X. Role of the carrier gas flow rate in monolayer MoS_2 growth by modified chemical vapor deposition. *Nano Res.* **2017**, *10*, 643−651.
(32) Raju, M.; Wan, M.; Sen, S.; Jacob, C. Influence of chemical potential on shape evolution of 2D-MoS_2 flakes produced by chemical vapor deposition. *Nanotechnology* **2021**, *32*, No. 045301.
(33) Chen, W.; Zhao, J.; Zhang, J.; Gu, L.; Yang, Z.; Li, X.; Yu, H.; Zhu, X.; Yang, R.; Shi, D.; Lin, X.; Guo, J.; Bai, X.; Zhang, G. Oxygen-Assisted Chemical Vapor Deposition Growth of Large Single-Crystal and High-Quality Monolayer MoS_2. *J. Am. Chem. Soc.* **2015**, *137*, 15632−15635.
(34) Kim, H.; Ovchinnikov, D.; Deiana, D.; Unuchek, D.; Kis, A. Suppressing Nucleation in Metal-Organic Chemical Vapor Deposition of MoS_2 Monolayers by Alkali Metal Halides. *Nano Lett.* **2017**, *17*, 5056−5063.
(35) Huang, Y.; Sutter, E.; Shi, N. N.; Zheng, J.; Yang, T.; Englund, D.; Gao, H. J.; Sutter, P. Reliable Exfoliation of Large-Area High-Quality Flakes of Graphene and Other Two-Dimensional Materials. *ACS Nano* **2015**, *9*, 10612−10620.
(36) Li, H.; Wu, J.; Yin, Z.; Zhang, H. Preparation and applications of mechanically exfoliated single-layer and multilayer MoS_2 and WSe_2 nanosheets. *Acc. Chem. Res.* **2014**, *47*, 1067−1075.
(37) Novoselov, K. S.; Jiang, D.; Schedin, F.; Booth, T. J.; Khotkevich, V. V.; Morozov, S. V.; Geim, A. K. Two-dimensional atomic crystals. *Proc. Natl. Acad. Sci. U.S.A.* **2005**, *102*, 10451−10453.
(38) Desai, S. B.; Madhvapathy, S. R.; Amani, M.; Kiriya, D.; Hettick, M.; Tosun, M.; Zhou, Y.; Dubey, M.; Ager, J. W., III; Chrzan, D.; Javey, A. Gold-Mediated Exfoliation of Ultralarge Optoelectronically-Perfect Monolayers. *Adv. Mater.* **2016**, *28*, 4053−4058.
(39) Li, Y. D.; Zhen, W. L.; Weng, S. R.; Hu, H. J.; Niu, R.; Yue, Z. L.; Xu, F.; Zhu, W. K.; Zhang, C. J. Interface effects of Schottky devices built from MoS2 and high work function metals. *J. Phys.: Condens. Matter* **2022**, *34*, No. 165001.
(40) Huang, Y.; Pan, Y. H.; Yang, R.; Bao, L. H.; Meng, L.; Luo, H. L.; Cai, Y. Q.; Liu, G. D.; Zhao, W. J.; Zhou, Z.; Wu, L. M.; Zhu, Z. L.; Huang, M.; Liu, L. W.; Liu, L.; Cheng, P.; Wu, K. H.; Tian, S. B.; Gu, C. Z.; Shi, Y. G.; Guo, Y. F.; Cheng, Z. G.; Hu, J. P.; Zhao, L.; Yang, G. H.; Sutter, E.; Sutter, P.; Wang, Y. L.; Ji, W.; Zhou, X. J.; Gao, H. J. Universal mechanical exfoliation of large-area 2D crystals. *Nat. Commun.* **2020**, *11*, No. 2453.
(41) Liu, F.; Wu, W.; Bai, Y.; Chae, S. H.; Li, Q.; Wang, J.; Hone, J.; Zhu, X. Y. Disassembling 2D van der Waals crystals into macroscopic monolayers and reassembling into artificial lattices. *Science* **2020**, *367*, 903−906.
(42) Velický, M.; Donnelly, G. E.; Hendren, W. R.; McFarland, S.; Scullion, D.; DeBenedetti, W. J. I.; Correa, G. C.; Han, Y.; Wain, A. J.; Hines, M. A.; Muller, D. A.; Novoselov, K. S.; Abruna, H. D.; Bowman, R. M.; Santos, E. J. G.; Huang, F. Mechanism of Gold-Assisted Exfoliation of Centimeter-Sized Transition-Metal Dichalcogenide Monolayers. *ACS Nano* **2018**, *12*, 10463−10472.
(43) Li, Z.; Ren, L.; Wang, S.; Huang, X.; Li, Q.; Lu, Z.; Ding, S.; Deng, H.; Chen, P.; Lin, J.; Hu, Y.; Liao, L.; Liu, Y. Dry Exfoliation of Large-Area 2D Monolayer and Heterostructure Arrays. *ACS Nano* **2021**, *15*, 13839−13846.
(44) Li, Z.; Lv, Y.; Ren, L.; Li, J.; Kong, L.; Zeng, Y.; Tao, Q.; Wu, R.; Ma, H.; Zhao, B.; Wang, D.; Dang, W.; Chen, K.; Liao, L.; Duan, X.; Duan, X.; Liu, Y. Efficient strain modulation of 2D materials via polymer encapsulation. *Nat. Commun.* **2020**, *11*, No. 1151.
(45) Sun, W.; Zhao, J.; Chen, S.; Guo, X.; Zhang, Q. Thermally cross-linked polyvinyl alcohol as gate dielectrics for solution

https://doi.org/10.1021/acsomega.2c04409
ACS Omega 2022, 7, 38774−38781

processing organic field-effect transistors. *Synth. Met.* **2019**, *250*, 73−78.
(46) Gorbachev, R. V.; Riaz, I.; Nair, R. R.; Jalil, R.; Britnell, L.; Belle, B. D.; Hill, E. W.; Novoselov, K. S.; Watanabe, K.; Taniguchi, T.; Geim, A. K.; Blake, P. Hunting for monolayer boron nitride: optical and Raman signatures. *Small* **2011**, *7*, 465−468.
(47) Reich, S.; Thomsen, C. Raman spectroscopy of graphite. *Philos. Trans. R. Soc., A* **2004**, *362*, 2271−2288.
(48) Stankovich, S.; Dikin, D. A.; Piner, R. D.; Kohlhaas, K. A.; Kleinhammes, A.; Jia, Y.; Wu, Y.; Nguyen, S. T.; Ruoff, R. S. Synthesis of graphene-based nanosheets via chemical reduction of exfoliated graphite oxide. *Carbon* **2007**, *45*, 1558−1565.
(49) Abhilash, T. S.; De Alba, R.; Zhelev, N.; Craighead, H. G.; Parpia, J. M. Transfer printing of CVD graphene FETs on patterned substrates. *Nanoscale* **2015**, *7*, 14109−14113.
(50) Cui, X.; Lee, G. H.; Kim, Y. D.; Arefe, G.; Huang, P. Y.; Lee, C. H.; Chenet, D. A.; Zhang, X.; Wang, L.; Ye, F.; Pizzocchero, F.; Jessen, B. S.; Watanabe, K.; Taniguchi, T.; Muller, D. A.; Low, T.; Kim, P.; Hone, J. Multi-terminal transport measurements of MoS_2 using a van der Waals heterostructure device platform. *Nat. Nanotechnol.* **2015**, *10*, 534−540.
(51) Dean, C. R.; Young, A. F.; Meric, I.; Lee, C.; Wang, L.; Sorgenfrei, S.; Watanabe, K.; Taniguchi, T.; Kim, P.; Shepard, K. L.; Hone, J. Boron nitride substrates for high-quality graphene electronics. *Nat. Nanotechnol.* **2010**, *5*, 722−726.
(52) Shiue, R. J.; Gao, Y.; Wang, Y.; Peng, C.; Robertson, A. D.; Efetov, D. K.; Assefa, S.; Koppens, F. H.; Hone, J.; Englund, D. High-Responsivity Graphene-Boron Nitride Photodetector and Autocorrelator in a Silicon Photonic Integrated Circuit. *Nano Lett.* **2015**, *15*, 7288−7293.
(53) Wang, L.; Meric, I.; Huang, P. Y.; Gao, Q.; Gao, Y.; Tran, H.; Taniguchi, T.; Watanabe, K.; Campos, L. M.; Muller, D. A.; Guo, J.; Kim, P.; Hone, J.; Shepard, K. L.; Dean, C. R. One-dimensional electrical contact to a two-dimensional material. *Science* **2013**, *342*, 614−617.
(54) Li, S.; Chen, X.; Liu, F.; Chen, Y.; Liu, B.; Deng, W.; An, B.; Chu, F.; Zhang, G.; Li, S.; Li, X.; Zhang, Y. Enhanced Performance of a CVD MoS_2 Photodetector by Chemical in Situ n-Type Doping. *ACS Appl. Mater. Interfaces* **2019**, *11*, 11636−11644.
(55) Hua, X.; Axenie, T.; Goldaraz, M. N.; Kang, K.; Yang, E. H.; Watanabe, K.; Taniguchi, T.; Hone, J.; Kim, B.; Herman, I. P. Improving the Optical Quality of $MoSe_2$ and WS_2 Monolayers with Complete h-BN Encapsulation by High-Temperature Annealing. *ACS Appl. Mater. Interfaces* **2022**, *14*, 2255−2262.
(56) Zhen, W.; Zhou, X.; Weng, S.; Zhu, W.; Zhang, C. Ultrasensitive, ultrafast and gate-tunable two-dimensional photodetectors in ternary rhombohedral ZnIn2S4 for optical neural networks. *ACS Appl. Mater. Interfaces* **2022**, *14*, 12571−12582.

https://doi.org/10.1021/acsomega.2c04409
ACS Omega 2022, 7, 38774−38781